Scalability as a Degree of Freedom in Electric Drive Train Simulation

Dominik Buecherl, *Student Member*, *IEEE*, Christiane Bertram, *Student Member*, *IEEE*, Andreas Thanheiser, *Student Member*, *IEEE*, and Hans-Georg Herzog, *Member*, *IEEE*
Institute for Energy Conversion Technology
Technische Universitaet Muenchen
Arcisstr. 21, 80333 Muenchen, Germany
Phone: +49-89-289-28424; Fax: +49-89-289-28335
EML: dominik.buecherl@tum.de

***Abstract*—Automotive companies are developing electric vehicles in different ways. There are several system topologies and component configurations used for prototype and mass production. To save time and money during the design process empirical values are necessary. In this paper, scalability is used as a powerful tool of electric drive train simulation. It enables the size variegation of drive train components like the electrical machine, the frequency inverter, and the energy storage. In addition, a novel scheme is derived for the control of rotating field machines in vehicular applications. The control strategy as well as the component configuration is optimized by a well-chosen method using scalability as degree of freedom. Closing, the several influences of component size variation and control parameterization on the drive train behavior is discussed.**

***Index Terms*—Scalability, electric drive train, electrical machine, frequency inverter, energy storage, control, optimization.**

I. Introduction

The development of electric drive trains is frequently discussed since almost every car manufacturer has started mass or prototype production of electric vehicles (EV) in the last years [1][2]. There are several electric drive train concepts – e.g. the search for adequate machine types [3]-[8] and storage technologies [9],[10] is well-known. Furthermore, the problem of a central or tandem drive versus a wheel-hub drive is often addressed. Nevertheless, researchers all over the world are looking for a uniform procedure used for configuring the drive train at an early stage of the design process [11].

Therefore, the engineering of future EVs requires extensive instruments for a premature and rough dimensioning of drive train components. This plays a decisive role especially for novel drive configurations like pure electric drive trains as there are no adequate empirical values yet in this area. For instance, one pivotal question of preliminary design is the interdependent dimensioning of the electrical machine, the frequency inverter and the energy storage. Several concepts and the search of the optimum configuration are discussed at the moment since there are still no proven results for the question what component sizes are optimal.

The goal of this current work is to use the approach of scalability as a degree of freedom for the stationary simulation of vehicular electric drive trains.

II. Approach

To analyze the impact of scalability on the stationary simulation and behavior of EVs a set of influences has to be considered. A systematic procedure must be used to tackle this complex problem. The following approach was developed to ensure a high-quality outcome:

Scalable simulation models: To variegate the size of several drive train components an extensive simulation model has to be built. For this purpose, the influence of scalability on the model accuracy of the electrical machine and the energy storage has to be figured out. The behavior of the inverter model has to be adapted towards the machine scaling.

Machine control: Firstly, the common control scheme of rotating field machines will be implemented in the simulation tool. Afterwards, an efficiency oriented control is derived and compared to the first scheme to find out what energy saving potential exists.

Optimization: To optimize the electric drive train an adequate optimization method has to be chosen. Furthermore, parameters in model scaling and control have to be defined to use them as degree of freedom for optimization.

Simulation runs: Using the scalable simulation models lots of simulation cycles are run to find out what influence the control scheme and component sizes have on drive train efficiency and thermal behavior.

III. Scalable Modeling

A. Energy storage

As energy storage a double-layer capacitor is modeled with the aid of an equivalent circuit considering the internal resistance as well as the self-discharge as it is shown in Figure 1. The capacitance is dependent on the voltage as it is mentioned in [10]. The properties of the single capacitor cell can be chosen arbitrary, i.e. capacitance, internal resistance, self-discharge, maximum voltage, cell weight, and SOC swing. The scalability is enabled by varying the number of cells in parallel or serial configuration. Other storage types (e.g. lithium iron phosphate, lithium cobalt oxide, nickel metal hydride) can also be simulated via equivalent circuits.

978-1-4244-8218-4/10/$26.00 ©2010 IEEE

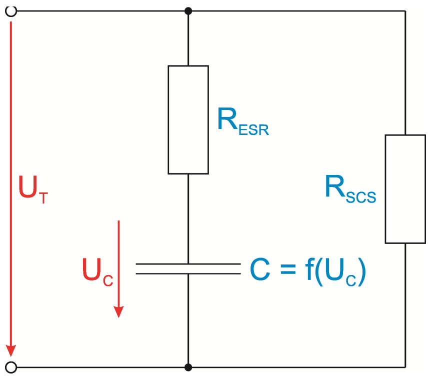

Figure 1 Equivalent circuit of a double-layer capacitor cell

B. *Electrical machine*

The electrical machine model also consists of an equivalent circuit showing an example in Figure 2. It includes the torque calculation at a given speed as well as ohmic and iron losses. Within the available study machine analyses and comparisons – especially for induction and synchronous machines – were made [4],[5]. This work is limited to asynchronous induction machines with squirrel cage rotor (IMSC) and permanent magnet synchronous machines (PMSM).

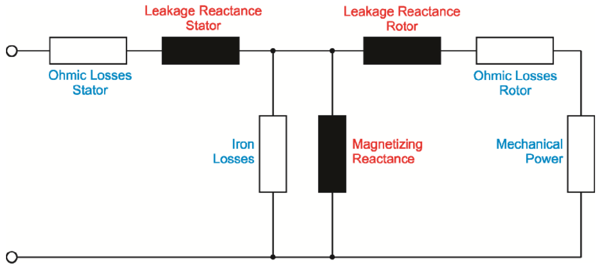

Figure 2 Equivalent circuit of an asynchronous induction machine

For induction machines with squirrel cage rotor, an extended equivalent circuit is used that was derived in [12] and is shown in Figure 3. The model considers iron losses, except those in the rotor. Equations for the estimation of necessary parameters can be found in [12].

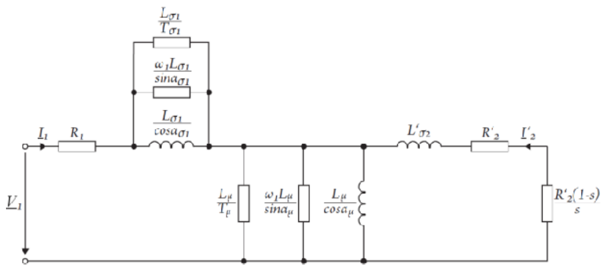

Figure 3 Extended equivalent circuit for asynchronous induction machines with squirrel cage considering iron losses

For permanent magnet synchronous machines, the extended equivalent circuit in Figure 4 is used that was also derived in [12] considering iron losses.

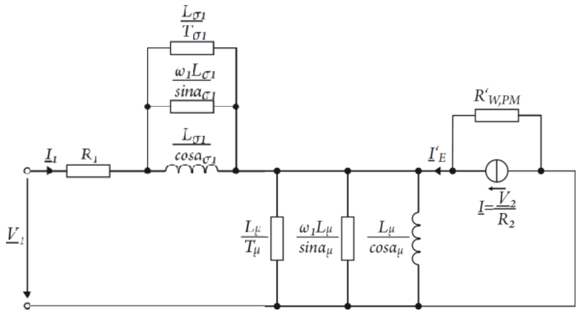

Figure 4 Extended equivalent circuit for permanent magnet synchronous machines considering iron losses

Scalability is implemented continuously variable by a geometric scaling of the machine's size. Therefore, two geometric scaling factors were established – k_a for the axial variation of the machine and k_r for the radial scale of the machine [13]. In this way, the size of the machine can be variegated provided that the basic construction, the type of cross-section as well as the cooling system remain unchanged.

The complete geometric scaling process is related to a reference machine that was designed for use in a vehicular electric drive train [4]. The scaling of the machine's size has influence on the mechanical behavior.

As the rated torque of an electrical machine is commensurate to its volume the machine's operating range is enlarged by increasing the scaling factor(s). Figure 5 shows the consequence of the described machine scaling.

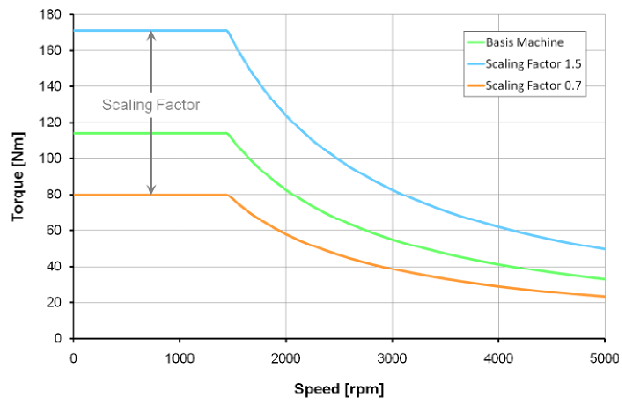

Figure 5 Influence of axial machine scaling on mechanical operating area depending on the axial scaling factor k_a

The scaling factors k_a and k_r are limited to the values given in Eq. 1 and 2 independent of the machine type.

$$0.5 \leq k_a \leq 2.0 \tag{1}$$
$$0.75 \leq k_r \leq 1.5 \tag{2}$$

The scaling influences on the machine behavior are derived in [13] resulting in equations that are shown in Tables I, II, III, and IV.

TABLE I.
INFLUENCE OF AXIAL SCALING ON IMSC PARAMETERS

Identifier	Description	Scaling influence
L_h	Magnetizing inductance	$L_{h,ka} = L_h \cdot k_a$
R_{Hh}	Hysteresis loss resistance belonging to magnetizing inductance	$R_{Hh,ka} = R_{Hh} \cdot k_a$
R_{Wh}	Eddy-current loss resistance belonging to magnetizing inductance	$R_{Wh,ka} = R_{Wh} \cdot k_a$
R_{1N}	Slot fraction of stator resistance	$R_{1N,ka} = R_{1N} \cdot k_a$
R_{1W}	End winding fraction of stator resistance	$R_{1W,ka} = const$
R'_{2N}	Slot fraction of transformed rotor resistance	$R'_{2N,ka} = R'_{2N} \cdot k_a$
R'_{2W}	End winding fraction of transformed rotor resistance	$R'_{2W,ka} = const$
$L_{\sigma N}$	Slot fraction of stator leakage inductance	$L_{\sigma N,ka} = L_{\sigma N} \cdot k_a$
$L_{\sigma W}$	End winding fraction of stator leakage inductance	$L_{\sigma W,ka} = const$

TABLE II.
INFLUENCE OF AXIAL SCALING ON PMSM PARAMETERS

Identifier	Description	Scaling influence
L_h	Magnetizing inductance	$L_{h,ka} = L_h \cdot k_a$
R_{Hh}	Hysteresis loss resistance belonging to magnetizing inductance	$R_{Hh,ka} = R_{Hh} \cdot k_a$
R_{Wh}	Eddy-current loss resistance belonging to magnetizing inductance	$R_{Wh,ka} = R_{Wh} \cdot k_a$
R_{1N}	Slot fraction of stator resistance	$R_{1N,ka} = R_{1N} \cdot k_a$
R_{1W}	End winding fraction of stator resistance	$R_{1W,ka} = const$
I'_E	Equivalent exciting current	$I'_{E,ka} = const$
R_{PM}	Magnet loss corresponding resistance	$R_{PM,ka} = R_{PM} \cdot k_a$
$L_{\sigma N}$	Slot fraction of stator leakage inductance	$L_{\sigma N,ka} = L_{\sigma N} \cdot k_a$
$L_{\sigma W}$	End winding fraction of stator leakage inductance	$L_{\sigma W,ka} = const$

TABLE III.
INFLUENCE OF RADIAL SCALING ON IMSC PARAMETERS

Identifier	Description	Scaling influence
L_h	Magnetizing inductance	$L_{h,kr} = const$
R_{Hh}	Hysteresis loss resistance belonging to magnetizing inductance	$R_{Hh,kr} = const$
R_{Wh}	Eddy-current loss resistance belonging to magnetizing inductance	$R_{Wh,kr} = const$
R_{1N}	Slot fraction of stator resistance	$R_{1N,kr} = \frac{R_{1N}}{k_r^2}$
R_{1W}	End winding fraction of stator resistance	$R_{1W,kr} = R_{1W} \cdot \frac{1}{k_r}$
R'_{2N}	Slot fraction of transformed rotor resistance	$R'_{2N,kr} = R'_{2N} \cdot \frac{1}{k_r^2}$
R'_{2W}	End winding fraction of transformed rotor resistance	$R'_{2W,kr} = R'_{2W} \cdot \frac{1}{k_r}$
$L_{\sigma N}$	Slot fraction of stator leakage inductance	$L_{\sigma N,kr} = const$
$L_{\sigma W}$	End winding fraction of stator leakage inductance	$L_{\sigma W,kr} = L_{\sigma W} \cdot k_r$

TABLE IV.
INFLUENCE OF RADIAL SCALING ON PMSM PARAMETERS

Identifier	Description	Scaling influence
L_h	Magnetizing inductance	$L_{h,kr} = const$
R_{Hh}	Hysteresis loss resistance belonging to magnetizing inductance	$R_{Hh,kr} = const$
R_{Wh}	Eddy-current loss resistance belonging to magnetizing inductance	$R_{Wh,kr} = const$
R_{1N}	Slot fraction of stator resistance	$R_{1N,kr} = \frac{R_{1N}}{k_r^2}$
R_{1W}	End winding fraction of stator resistance	$R_{1W,kr} = R_{1W} \cdot \frac{1}{k_r}$
I'_E	Equivalent exciting current	$I'_{E,kr} = I'_E \cdot k_r$
R_{PM}	Magnet loss corresponding resistance	$R_{PM,kr} = const$
$L_{\sigma N}$	Slot fraction of stator leakage inductance	$L_{\sigma N,kr} = const$
$L_{\sigma W}$	End winding fraction of stator leakage inductance	$L_{\sigma W,kr} = L_{\sigma W} \cdot k_r$

The resulting equivalent circuit models for IMSC and PMSM depending on scaling factors k_a and k_r are shown in Figure 6 and Figure 7 where ohmic and iron losses are considered [13].

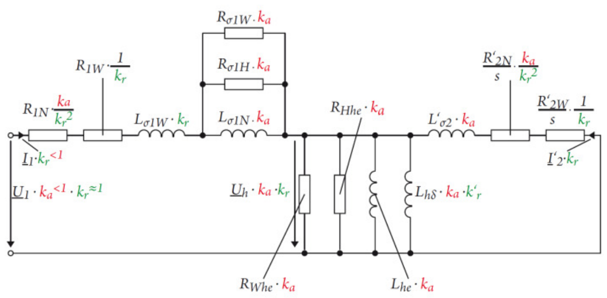

Figure 6 Scalable IMSC equivalent circuit

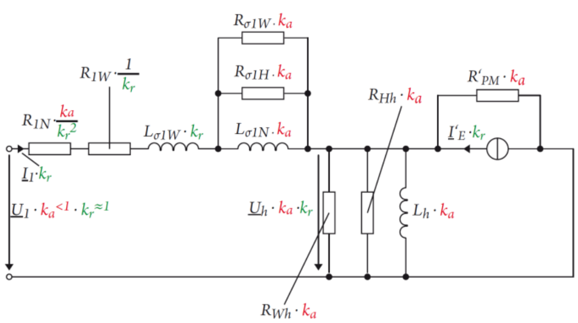

Figure 7 Scalable PMSM equivalent circuit

C. *Frequency inverter*

The frequency inverter model consists of analytical equations that calculate the diverse losses (e.g. ohmic losses, switching losses) and that are derived in [14]. The inverter is automatically adapted to the electrical machine's scaling. Furthermore, it considers the energy storage's voltage level during machine operation according to torque drawbacks.

IV. Machine Control

A. *Constant voltage-to-frequency ratio*

In a first step, the common control scheme for rotating field machines was implemented in the scalable simulation model. As the machine's rotating speed is below its rated speed the ratio of inverter output voltage and frequency is constant reaching rated voltage at rated frequency. For higher speed and frequency the voltage is controlled constant at the rated value, the so called field-weakening area.

Even if the control scheme is well-known and simple the control algorithm in the scalable simulation will be challenging. This is caused by the different mechanical machine behavior after scaling. An example is given in Figure 8 where the machine torque is shown against the machine speed for an asynchronous induction machine with squirrel cage. Here, three different radial scaling factors k_r are used. It becomes obvious that the linear area of the machine's operating curve changes its gradient according to the scaling factor. This influence is considered by the control scheme.

B. *Efficiency-oriented control*

State-of-the-art of machine control is the abovementioned scheme. But there is no constraint disabling another control method. Another applied approach for machine control is a control scheme that is addressing the drive train efficiency. For every mechanical operating point, the algorithm is able to offer the optimum voltage and frequency values to enable the best overall drive train efficiency considering storage, power electronics and machine losses.

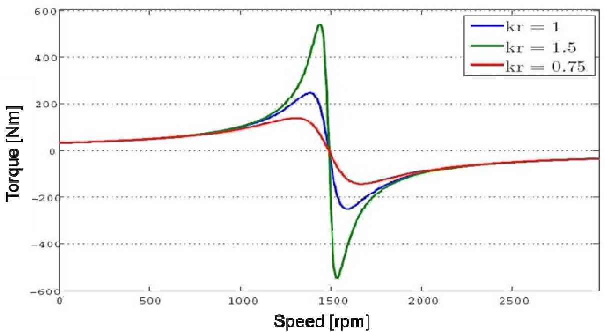

Figure 8 Influence of radial machine scaling on the IMSC's speed-torque-characteristics depending on scaling factor k_r

V. Optimization

The goal of the optimization process is to use the scalability of the drive train model as degree of freedom and to find the best configuration under given constraints. Therefore, the drive train model has to be parameterized. Parameters can be defined in the machine control for example. Another parameter can be the number of cells of the energy storage. Thus, the vehicle's energy content can be variegated. Further parameters can be represented by the two geometric scaling factors of the electrical machine k_a and k_r. The cost function of the optimization process is the drive train's energy consumption.

To get not only the optimum result but also to recognize system influences by trends, the optimization procedure was defined as a two-level method. Figure 9 shows the schematic diagram of the applied two-level optimization. The inner core of the procedure is represented by the scalable drive train simulation containing the abovementioned models. Input values for a driving cycle simulation is the energy storage size and control strategy parameters respectively. An optimization algorithm varies the input values dependent on the cost function completion (Level 2). On the upper level the drive train's hybridization factor is variegated by another optimization algorithm changing the machine's scaling factors (Level 1).

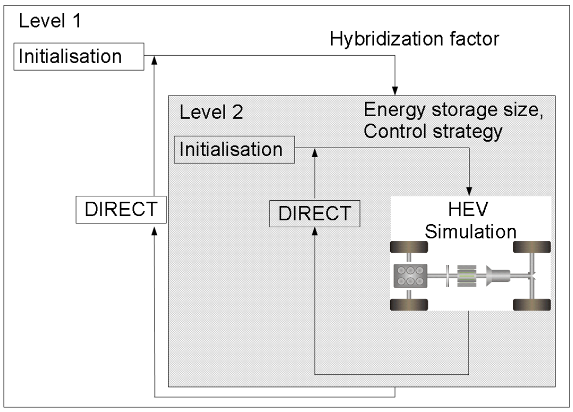

Figure 9 Schematic structure of the applied two-level optimization procedure

From a large number of optimization algorithms (e.g. genetic algorithms, particle swarm optimization) the so called DIRECT algorithm (dividing rectangles) was chosen as it goes well with electric drive train optimizations [3].

VI. Simulation Results

Lots of simulation runs were completed using the presented scalable drive train model. Several simulation results will be shown and discussed. For example the influence of control optimization (according to drive train efficiency) on the drive train behavior is presented. An example is represented by the drive train application within a parallel hybrid electric vehicle, as it is shown in Figure 10. Here, a machine type comparison of permanent magnet synchronous machine (PMSM) and asynchronous induction machine with squirrel cage (IMSC) is extended by an IMSC efficiency-oriented control.

Here, the abovementioned efficiency-optimized machine control scheme improves the IMSC operation behavior in a way that the IMDC is competitive with the PMSM with regard to the vehicle's fuel consumption even though the IMSC's maximum efficiency is clearly lower than the PMSM's.

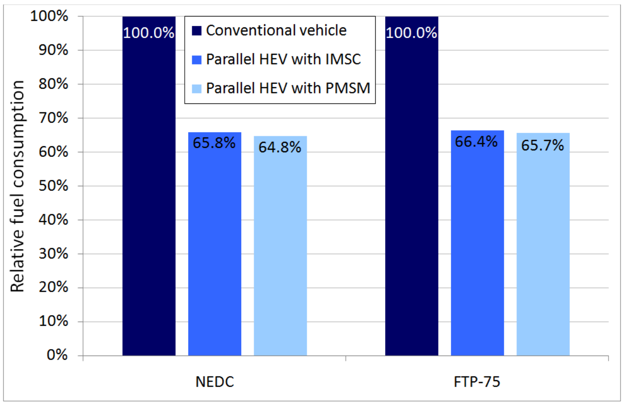

Figure 10 Relative fuel consumption of a hybrid electric vehicle during New European Driving Cycle and FTP-75 Driving Cycle

Influences of the energy storage and the hybridization factor (i.e. machine divided by engine power) on the drive train behavior can be analyzed using the scalable simulation. Figure 11 shows the vehicle's fuel consumption identifying also trend gradients enabled by the two-level procedure. In doing so, the optimum drive train configuration becomes visible.

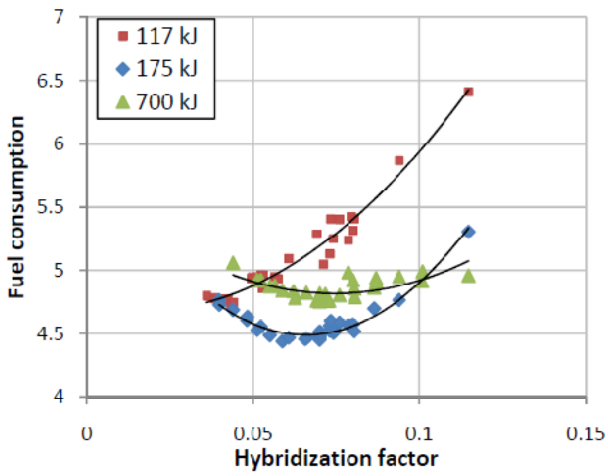

Figure 11 Influence of hybridization factor and energy storage size on fuel consumption (Middle class car, New European Drive Cycle)

VII. Conclusion

The present paper shows that a scalability-based drive train simulation describes a good uniform procedure for the configuration of electric drive trains in an early stage of design. For this purpose, a full drive train simulation model including scalable components like electrical machine, inverter, and energy storage was built and applied in a developed two-level optimization procedure. Several control strategies for the drive train and the electrical machine were used in a parameterized manner. In doing so, one is able optimize an electric drive train under given constraints and identify correlations by trends.

References

[1] D. Buecherl, I. Bolvashenkov, and H.-G. Herzog, "Verification of the Optimum Hybridization Factor as Design Parameter of Hybrid Electric Vehicles," in Proceedings of the IEEE Vehicle Power and Propulsion Conference (VPPC) 2009, pp. 847-851, 2009.

[2] I. Bolvashenkov and H.-G. Herzog, "System Approach to a Choice of Optimum Factor of Hybridization of the Electric Vehicle," in Proceedings of the EVS, 22nd International Battery, Hybrid and Fuel Cell Electric Vehicle Symposium & Exposition, 2006.

[3] D. W. Gao, C. Mi, and A. Emadi, "Modeling and Simulation of Electric and Hybrid Vehicles," in Proceedings of the IEEE, vol. 95, no. 4, pp. 729-745, 2007.

[4] D. Buecherl, R. Nuscheler, W. Meyer, and H.-G. Herzog, "Comparison of Electrical Machine Types in Hybrid Drive Trains: Induction Machine vs. Permanent Magnet Synchronous Machine," in Proceedings of the ICEM '08, XVIII International Conference on Electrical Machines, 2008.

[5] D. Bucherl, W. Meyer, and H.-G. Herzog, "Simulation of the Electrical Machine's Fuel Saving Potential in Parallel Hybrid Drive Trains," in Proceedings of the IEEE International Electric Machines and Drives Conference (IEMDC) 2009, pp. 653-660, 2009.

[6] A. Emadi, Y.J. Lee, and K. Rajashekara, "Power Electronics and Motor Drives in Electric, Hybrid Electric, and Plug-In Hybrid Electric Vehicles," in IEEE Transactions on Industrial Electronics, vol. 55, no. 6, pp. 2237-2245, 2008

[7] H. Neudorfer, "Comparison of three different electric powertrains for the use in high performance Electric Go-Kart," in Proceedings of the International Aegean Conference on Electrical Machines and Power Electronics (ACEMP), pp. 21-26, 2007.

[8] H. Neudorfer, N. Wicker, and A. Binder, "Comparison of Three Different Electric Powertrains for the Use in Hybrid Electric Vehicles," in Proceedings of the 4th IET Conference on Power Electronics, Machines and Drives (PEMD), pp. 510-514, 2008.

[9] A. Burke, "Batteries and Ultracapacitors for Electric, Hybrid, and Fuel Cell Vehicles," in Proceedings of the IEEE, vol. 95, no. 4, pp. 806-820, 2007.

[10] T. Kohler, D. Buecherl, and H.-G. Herzog, "Investigation of Control Strategies for Hybrid Energy Storage Systems in Hybrid Electric Vehicles," in Proceedings of the IEEE Vehicle Power and Propulsion Conference (VPPC) 2009, pp. 1687-1693, 2009.

[11] D. Buecherl and H.-G. Herzog, "Scalable Simulation for Preliminary Design of Electrified Power Trains," in Proceedings of the 5th IET Conference on Power Electronics, Machines and Drives (PEMD) 2010.

[12] D. Buecherl and H.-G. Herzog, "Iron Loss Modeling by Complex Inductances for Steady State Simulation of Electrical Machines," in Proceedings of the 20th International Symposium on Power Electronics, Electrical Drives, Automation and Motion (SPEEDAM) 2010, pp. 878-883, 2010.

[13] D. Buecherl and H.-G. Herzog, "Geometric Scaling and its Effects on Steady-State Simulation of Rotating Field Machines," accepted paper at the XIX International Conference on Electrical Machines (ICEM) 2010.

[14] R. Nuscheler, W. Meyer, and M. Schmid. „Efficiency-Optimized Simulation of Asynchronous Machines Combined with PWM Converters," in Proceedings of the 16th International Conference on Electrical Machines (ICEM), 2004.